Jusami
Homepage: http://jusami.batan.go.id
Jurnal Sains Materi Indonesia
Akreditasi LIPI No.: 395/D/2012
Tanggal 24 April 2012
ISSN: 1411-1098

X-RAYS DIFFRACTION STUDY ON THE IRON NANOPARTICLES PREPARED BY TWO STEP MILLING METHOD

Engkir Sukirman and Yosef Sarwanto
Center for Technology of Nuclear Industry Materials - Indonesian National Nuclear Energy Agency
Kawasan Puspiptek, Serpong 15314, Tangerang Selatan
e-mail**:** engkirs@gmail.com

Recived: 7 Juni 2013 *Reviewed: 20 September 2013* *Accepted: 21 November 2013*

ABSTRACT

X-RAYS DIFFRACTION STUDY ON THE IRON NANOPARTICLES PREPARED BY TWO STEPS MILLING METHOD. X-rays diffraction study on the iron nanoparticles prepared by two-step milling method has been carried out. First, the raw material of micro-sized Fe was crushed by High Energy Milling (HEM) in the presence of isopropyl alcohol, hereinafter referred to as FI precursor. FI precursor then was crushed again with planetary balls mill in Cetyl-Trimethyl-Ammonium Bromide (CTAB) media, hereinafter referred to as FC sample. The phases analysis in the two samples were carried out by X-rays diffraction technique using the Rietveld method. Crystallites size were calculated with the Debye-Scherrer formula and the size of particles were measured by means of Particles Size Analyzer (PSA). The magnetic properties of the two samples were characterized with Vibration Sample Magnetometer (VSM). The analysis result showed that each of FI and FC samples consist of Fe, γ-Fe_2O_3 and Fe_3O_4 phases in the form of the nano-sized powder ranging from around 7 to 10 nm. PSA data indicate that the particle size of FI and FC are the same, i.e., 7.5 nm with narrow size distribution. The VSM data revealed that both FI and FC samples display superparamagnetic behavior at room temperature. The magnetization value in FC sample has been reduced due to more of the mass fraction of Fe transforms into iron oxide phases. The particle size is generally not the same as the size of the crystallites and in particular for the nano-sized particles, the size of crystallites could be equal to or greater than the particle size due to the presence of polycrystalline aggregates.

Keywords**:** X-rays diffraction, Iron nanoparticles, Two step milling

ABSTRAK

STUDI DIFRAKSI SINAR-X PADA PARTIKEL NANO BESI HASIL PROSES *MILLING* DUA LANGKAH. Studi difraksi sinar-X pada partikel besi berukuran nano-meter telah dilakukan dengan metode *milling* dua langkah. Pertama, bahan baku Fe berukuran mikro meter digerus menggunakan alat *High Energy Milling* (*HEM*) di dalam media isopropil alkohol, selanjutnya disebut prekursor FI. Prekursor FI kemudian digerus lagi dengan *planetary balls mill* di dalam media *Cetyl-Trimethyl-Ammonium Bromide* (*CTAB*), selanjutnya cuplikan disebut FC. Analisis fasa-fasa di dalam kedua cuplikan dilakukan dengan teknik difraksi sinar-X menggunakan metode *Rietveld*. Ukuran kristalit dihitung dengan rumus Debye-Scherrer dan ukuran partikel diukur menggunakan *Partikel Size Analyzer* (*PSA*). Sifat magnetik kedua cuplikan dikarakterisasi dengan *Vibration Sample Magnetometer* (*VSM*). Hasil analisis menunjukkan bahwa masing-masing cuplikan FI dan FC terdiri dari fasa Fe, γ-Fe_2O_3 dan Fe_3O_4 dalam bentuk serbuk nano yang berukuran sekitar 7 nm hingga 10 nm. Data PSA menunjukkan bahwa ukuran partikel FI dan FC adalah sama, yaitu 7,5 nm dengan distribusi ukuran yang sempit. Data *VSM* mengungkapkan bahwa kedua cuplikan FI dan FC menampilkan perilaku superparamagnetik pada suhu kamar. Magnetisasi cuplikan FC telah menyusut akibat lebih banyak fraksi massa Fe yang berubah menjadi fasa besi oksida. Ukuran partikel umumnya tidak sama dengan ukuran kristalit dan khususnya untuk partikel berukuran nano, ukuran kristalit bisa sama atau lebih besar dari ukuran partikel karena adanya agregat (tumpukan) polikristalin.

Kata kunci: Difraksi sinar-X, Partikel nano besi, *Milling* dua langkah

INTRODUCTION

Research and development of magnetic nanoparticles (NPs) have been carried out all over the world due to these NPs have potential applications in many biological and biomedical applications such as magnetic resonance imaging, targeted drug delivery, and magnetic fluid hyperthermia [1-3]. Biomedical applications require magnetic nanoparticles with size smaller than 20 nm, a narrow size distribution, water

soluble, and biocompatible [4]. For biological and biomedical applications, magnetic iron oxide nanoparticles are the primary choice because of their biocompatibility and chemical stability [5].

The magnetic NPs are suitable for biological and biomedical application, due to: (1) The magnetic NPs can be selectively separated (removed) from the complex samples using an external magnetic field. This process is very important for bio applications due to the fact that absolute majority of biological materials have diamagnetic properties which enable efficient selective separation of magnetic materials [2]. The magnetic NPs can be targeted to the desired place and kept there using an external magnetic field. These properties can be used e.g. for sealing the rotating objects or in the course of magnetic drug targeting. (3) The magnetic NPs can generate heat when subjected to high frequency alternating magnetic field; this phenomenon is employed especially during magnetic fluid hyperthermia (e.g., for cancer treatment). (4) The magnetic NPs generate a negative T2 contrast during magnetic resonance imaging thus serving as efficient contrast agents [5]. The magnetic NPs can be used for magnetic modification of diamagnetic biological materials, organic polymers and inorganic materials, and for magnetic labeling of biologically active compounds (e.g. antibodies, enzymes, aptamers, etc.). The magnetic NPs mentioned above have super paramagnetic properties.

To obtain magnetic NPs, there are many ways have been researched and developed and can be broadly classified into two categories: top-down and bottom-up methods [6]. The first category is to start with a bulk material and then break it into smaller pieces using mechanical, chemical or other form of energy. The second category is to synthesize the material from atomic or molecular species via chemical reactions, allowing for the precursor particles to grow in size. In this experiment, the magnetic NPs were synthesized with the top-down methods using High Energy Milling (HEM) process. The first category was chosen because it is simpler, cheaper, and easier than the second one.

In the previous investigation [7] the iron nanoparticle was synthesized by high-energy balls milling. Fe powder of high purity (99.9%, Alfa-Aesar Co.) was used as starting material. The particle size was approximately 5 μm in diameter. HEM was carried out at room temperature using a vibratory mill (SPEX 8000 mixer). An argon-flushed glove box used to prevent oxidation during balls milling was employed. A balls to powder (BTP) weight ratio was 10:1, and milled for 30 h. High Resolution Scanning Electron Microscope (HR-SEM) images confirmed the nanoparticles presence with approximately 2–4 nm in size. It was found that using this method allowed the formation of nanoparticles in a smaller size range than other synthesis methods.

The previous paper [8] presented the results of iron-NPs preparation using HEM process on micro size Fe powder in the media mix of ethanol and water (volume ratio 10:1). The phase analysis on the X-rays diffraction pattern using Rietveld analysis method showed the formation of mixture phase of Fe, Fe_3O_4, and γ-Fe_2O_3 of amount 55.8, 32.6 and 11.5 weight percent, respectively. The particle size of Fe, Fe_3O_4, and γ-Fe_2O_3 were calculated by using Debye-Scherrer formula based on X-rays diffraction data with the results of 11.8, 11.0 and 11.9 nm, successively. The lattice parameters of Fe, Fe_3O_4, and γ-Fe_2O_3 after Rieveld refinement are 2.888(6), 8.471(1), and 8.310(6) Å, respectively. So, by milling, in addition to grain size reduction from micro to nano size, there is also a phase transformation of approximately 44% Fe to Fe_3O_4 and γ-Fe_2O_3.

In contrast to previous studies, in which the milling process was only carried out in one stage, in this research, we prepared iron NPs by crushing the micrometer size iron powder in two steps, firstly using high energy milling in the presence of isopropyl alcohol and secondly using planetary balls mill In Cetyl-Trimethyl-Ammonium Bromide (CTAB) media. The purpose of milling in alcohol media is to minimize oxidation. While CTAB serves as surfactant inhibit particle clotting [9]. Therefore, it is expected that after the iron nanoparticles formed in the first step, the weight percent of iron oxides on the second step increase and the size of the iron nanoparticles are not getting bigger due to clotting.

The purpose of this research is to do the X-rays diffraction study in (1) identifying the qualitative and quantitative phases formed after the milling process, (2) knowing crystallite size of magnetic NPs associated with magnetic properties. Those physical properties are very important in the future-practical application.

EXPERIMENTAL METHODE

Commercially Fe powder (Merck product) with 99.5 % purity and particle size of 10 μm were used as a basic ingredient for preparing the Fe nanoparticles. 40 ml isopropyl alcohol, C_3H_8O (Merck product) with 99.7 % purity was poured into a vial containing 30 g of the Fe powder. Then, 10 balls with weight of 15 g of each were inserted into the vial in order to achieve the BTP weight ratio of 5:1. The milling vial and the balls were made from hardened steel (medium or high carbon steel). The raw material was crushed using High Energy Milling (HEM) SPEX 8000.

Milling process and handling of the starting powder and the milled particles were carried out in an atmosphere environment. To avoid overheating, HEM was operated in two cycles, namely cycles ON and OFF for 2.0 and 0.5 hours, respectively. At the first step, milling was carried out by HEM in

is opropyl alcohol medium for 40 hours with the aim to control the oxidation process. The milling result was called as FI. After being dried, the FI precursor was crushed by planetary balls mill in medium of Cetyl-Trimethylammonium Bromide (CTAB) for 40 hours.

The purpose of this second step was not only to reduce the particle size but also to increase of the weight fraction of iron oxides. So that the magnetization changes on the sample can be seen with tangible. The use of CTAB medium was intended to prevent agglomeration of those particles throughout the process. Then, the sample produced in the second step was called FC. The CTAB used have the chemical formula of $C_{19}H_{42}BrN$ produced by Merck with purity of pro-analysis. The BTP weight ratio was also 5:1. The CTAB solution used is 1 % weight per volume.

The samples characterization was determined by means of XRD (X-rays diffractometer) of PANalitical Xpert-Pro. Measurements were made in the 2θ angle range of 10°-80°, using the Cu target, X-rays wavelength: λ = 1.5406 Å, step width: 0.02°, and preset-time: 0.05 seconds. X-rays diffraction data were analyzed by the Rietveld method using the software RIETAN [10]. Debye-Scherrer formula [11] is employed for estimating crystallite size.

The particle size distributions were determined by PSA (Particle Size Analyzer) made by Malvern. Meanwhile, the magnetic properties of materials were characterized using Vibrating Sample Magnetometer (VSM) Oxford Type 1.2 H. Measurement of magnetic properties of materials was made in an applied magnetic field to a maximum value of 1 Tesla. All measurements (XRD, PSA, and VSM) were carried out at room temperature.

RESULTS AND DISCUSSIONS

The X-rays diffraction data were analyzed by the Rietveld method [10]. The refinement of the two types of sample was carried out by assuming that each of the sample contains three phases, i.e., Fe, γ-Fe_2O_3, and Fe_3O_4 with space group: Im3m (Vol. I, No. 229), P4132 (Vol. I, No. 213), and Fd3m (Vol. I, No. 227), respectively The atomic coordinate fraction of Fe, γ-Fe_2O_3, and Fe_3O_4 phases are illustrated in Table 1, 2 and 3, respectively [12].

The Rietveld refinement results based on X-rays diffraction pattern of FI, and FC samples are shown in Figures 1 and 2, respectively. The observed profiles are indicated by the dots and the calculated profiles are described by solid lines; vertical short lines indicate the position of Bragg peaks. Under the vertical short lines is the deviation profile between the observed and calculated intensities. It is shown in the figures that almost all of the calculated diffraction profile coincides with the observed diffraction pattern.

Table 1. The atomic coordinate fraction (xj, yj, zj) and occupation factor (gj) of Fe phase

	Occupation factor	Atomic coordinate fraction		
Atom	g_j	x_j	y_j	z_j
Fe^{3+}(1)	0.5	0.0	0.0	0.0
Fe^{3+}(2)	0.5	0.5	0.5	0.5

Table 2. The atomic coordinate fraction (xj, yj, zj) and occupation factor (gj) of g-Fe_2O_3 phase

	Occupation factor	Atomic coordinate fraction		
Atom	g_j	x_j	y_j	z_j
Fe^{3+}(1)	1.0	0.9975	0.9975	0.9975
Fe^{3+}(2)	1.0	0.8684	0.6184	0.875
Fe^{3+}(3)	1.0	0.375	0.125	0.875
O^{2-}(1)	1.0	0.389	0.389	0.389
O^{2-}(2)	1.0	0.377	0.368	0.865

Table 3. The atomic coordinate fraction (xj, yj, zj) and occupation factor (gj) of of Fe_3O_4 phase

	Occupation factor	Atomic coordinate fraction		
Atom	g_j	x_j	y_j	z_j
Fe^{3+}(A)	1.0	0.0	0.0	0.0
Fe^{3+}(B)	0.5	0.625	0.625	0.625
Fe^{2+}(B)	0.5	0.625	0.625	0.625
O	1.0	0.375	0.375	0.375

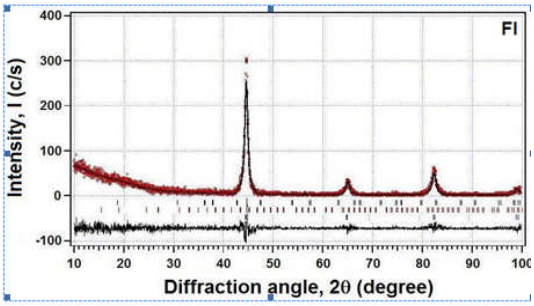

Figure 1. The Rietveld refinement results based on X-rays diffraction patterns of FI samples

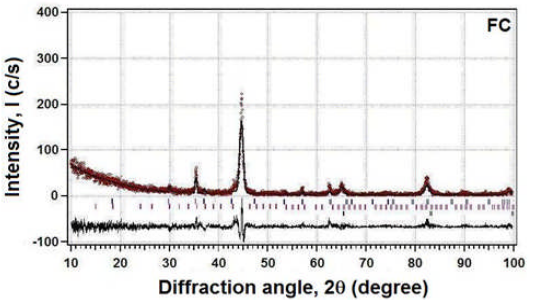

Figure 2. The Rietveld refinement results based on X-rays diffraction patterns of FC samples

The calculations were carried out step by step as follows: Iteration-1, refinement on the background counts parameters (b_0, b_1, ..., b_9) and scale factor (s) were carried out. Iteration-2, refinement on the FWHM parameter (U, V, W), and Lorentzian factor (X, Y) were done. Iteration-3, refinement on the lattice parameters (a, b, c) was performed. Iteration-4, scale factor (s) and preferred orientation factor (p) were refined. Iteration-5, the atomic occupation factor

parameters (g_j), the atomic coordinate fraction (x_j, y_j, z_j) and temperature parameters (Q_j) were refined Iteration-6, 7, 8, and so do the smoothing for all parameters simultaneously.

While the execution of the program, both on samples FI and FC stopped at the fourth iteration due to the matrix were not positive definite (NDP). Thus, the coordinate fraction parameters and occupation factors of the atoms can not be refined. However, the goodness of fitting called S factor, for FI and FC samples were 1.159, and 1.174, respectively. It appears that the S factors are smaller than the standard required, i.e., S = 1.3. Thus, the atomic coordinate fractions though not being refined have indicated the right values. The reliability index (R factors) [10] for the FI and FC samples were shown in Table 4 and 5.

Table 4. The reliability indexs, R_{WP}, R_p and S for the FI and FC samples

Sample	R_{WP}	R_P	S
FI	27.86	20.30	1.159
FC	29.71	22.00	1.174

Table 5. The reliability indexs, RI and RF for Fe, g-Fe2O3 and Fe3O4 each in FI and FC samples.

		Sample	
Phase	Parameter	FI	FC
Fe	R_I	15.24	16.18
	R_F	10.29	10.52
γ-Fe_2O_3	R_I	38.61	32.88
	R_F	33.76	18.65
Fe_3O_4	R_I	33.14	32.97
	R_F	20.88	18.90

Table 6. Lattice parameter (*a*, *b*, *c*) and mass fraction (*M*) in FI and FC samples

		Sample	
Phase	Parameter	FI	FC
Fe	$a = b = c$ (Å)	2.891(1)	2.888(1)
	M (%)	86	67
γ-Fe_2O_3	$a = b = c$ (Å)	8.328(4)	8.41(1)
	M (%)	12	11
Fe_3O_4	$a = b = c$ (Å)	8.42(2)	8.47(1)
	M (%)	2	22

The Rietveld refinement results based on X-rays diffraction patterns were shown in Table 6. Numbers in brackets are the accuracy imposed on the last digit after the decimal point. As shown in Table 6 that the samples are still dominated by iron phase, but the iron phase content reduced from 86 % in FI to 67 % in FC. On the contrary, magnetite phase increased significantly from 2 % in FI to 22 % in FC and maghemite phase slightly decreased from 12 % in FI to 11 % in FC. Thus, milling in CTAB medium converts iron more into iron oxides.

The formation mechanism of iron nanoparticles and iron oxides are assumed as follows. With increasing milling time, the particles size of iron powder will be smaller. The smaller the iron powder, the more easily it is oxidized to be iron oxide nanoparticles. Therefore the formation of iron and iron oxide nanoparticles occur when milling.

Origins of diffraction line broadening are crystallite size, strains, and instrumental broadening. If there were no crystallite size, strains, and instrumental broadening, then diffraction pattern will consist of vertical lines. Crystallite size determination is one of the most important topics in materials science research. Unfortunately crystallite size is a quantity, which cannot be directly measured. In addition there is an enormous confusion in literature concerning the definition of particle size, crystal size or grain size, and crystallite size. It is important to note that the particle size is always the largest, and may consist of several crystals or grains and perhaps even grains of different materials. A grain can be crystalline, (i.e., single crystalline or poly-crystalline) or amorphous. The single crystal grains can be distinguished from polycrystalline grains, in which a single crystal grain will form a sharp diffraction pattern associated with that material, while the polycrystalline grains will consist of many diffraction peaks [13, 14].

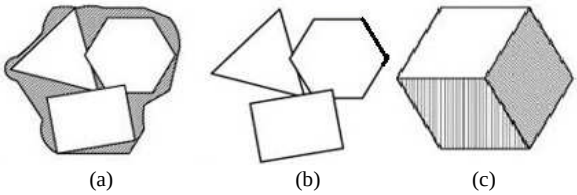

Figure 3. Schematic representation of terms: (a) particle size, (b) crystal size (grain size), and (c) crystallite size [15].

It is important to realize, that particle size cannot be determined by powder diffraction. Typical methods used for particle size determination are TEM, PSA, and others. Crystal size or grain size is not accessible by powder diffraction as well. Methods for crystal size determination are the same as for particle size determination. The size of a crystal or grain is in general equal or less than the particle size. Crystallites are the crystalline regions of material which scatter the X-rays or neutron beams coherently. A crystallite is long range order of atoms. An individual crystallite consists of a single phase. They are single crystal in nature. The method commonly used for crystallite size determination is XRD. However, in nanoparticles it is found a good agreement between particle size obtained from TEM and crystallite size obtained from XRD analysis. Schematic representation of terms: (a) particle size, (b) crystal size, and (c) crystallite size are indicated in Figure 3 [15, 16].

As mentioned above, crystallite size can be determined by means of XRD indirectly, provided that instrumental broadening is corrected first. For the correction of instrumental broadening, a silicon standard sample with negligible size and strain broadening was run. The peak broadening of the

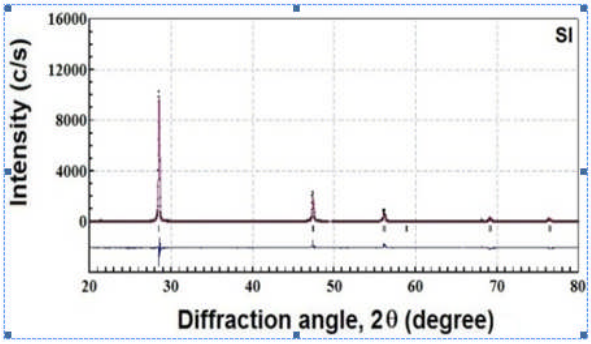

Figure 4. The X-rays diffraction pattern of Si standard sample that has been analyzed by the Rietveld method.

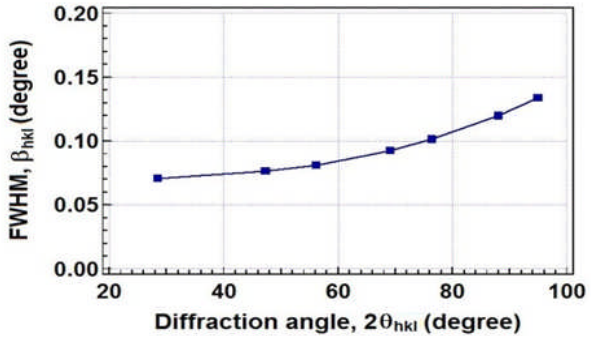

Figure 5. Graph of full width at half maximum, versus the scattering angle, 2θ of standard Si sample.

standard sample is exactly the instrumental broadening.

The X-rays diffraction pattern of Si standard sample after being refined by the Rietveld method is shown in Figure 4 with the reliability index, R_{wp}, R_p and S are 38.60, 31.05 and 1.984, respectively. The Si standard sample used in this experiment is in powder form. The graph showing the relationship between FWHM, β_{hkl} and the scattering angle, $2\theta_{hkl}$ of the Si standard sample is indicated in Figure 5, where the graph satisfies the equation:

$$Y = 9\times10^{-8}X^3 - 2\times10^{-6}X^2 + 3\times10^{-5}X + 0.069 \quad \text{..... (1)}$$

where $Y = \beta_{hkl}$ and $X = 2\theta_{hkl}$ with an error factor $R^2 = 1$. Thus, Equation (1) is actually the peak broadening due to instrument, $(\beta_{hkl})_{instrumental}$. The instrumental broadening, then, is used to correct the measured peak broadening, $(\beta_{hkl})_{refined}$ using the relation :

$$\beta_{hkl} = [(\beta_{hkl})^2_{refined} - (\beta_{hkl})^2_{instrumental}]^{1/2} \quad \text{..... (2)}$$

Therefore, β_{hkl} in Equation (2) is the peak broadening due to crystallite size and strain broadening. The generally accepted method to estimate the mean crystallite size of nanoparticles is Debye-Scherrer formula [11], as follows:

$$D_{hkl} = \frac{0.9\lambda}{\beta_{hkl}\cos\theta_{hkl}} \quad \text{..... (3)}$$

where:

D_{hkl} = Crystallite size

λ = X-rays wavelength

θ_{hkl} = Bragg angle of (hkl)-reflection plane

Table 7. The (bhkl)refined data from Si sample.

Phase	(hkl)	2θ (°)	$(\beta_{hkl})_{refined}$ (°)
Si	(111)	28.440	0.0710
	(220)	47.298	0.0763
	(311)	56.117	0.0813
	(400)	69.123	0.0927
	(331)	76.368	0.1014
	(422)	88.020	0.1198
	(333)	94.941	0.1337

Table 8. The $(\beta_{hkl})_{refined}$ data from FI sample.

Phase	(hkl)	2θ (°)	$(\beta_{hkl})_{refined}$ (°)	D_{hkl}(nm)
Fe	(110)	44.266	0.7016	12.3
	(200)	64.391	1.1159	8.4
	(211)	81.469	1.9342	5.4
γ-Fe_2O_3	(111)	18.437	1.3473	6.0
	(210)	23.872	1.1786	6.9
	(220)	30.331	0.9876	8.4
	(222)	37.375	0.8073	10.4
	(400)	43.428	0.7084	12.1
Fe_3O_4	(220)	29.958	0.9982	8.3
	(311)	35.285	0.8560	9.8
	(400)	42.880	0.7139	12.0

Table 9. The $(\beta_{hkl})_{refined}$ data from FC sample

Phase	(hkl)	2θ (°)	$(\beta_{hkl})_{refined}$ (°)	D_{hkl}(nm)
Fe	(110)	44.307	0.6734	12.8
	(200)	64.455	1.2216	7.7
	(211)	81.557	2.1817	4.8
γ-Fe_2O_3	(111)	18.242	1.6513	4.9
	(210)	23.618	1.4206	5.7
	(220)	30.006	1.1509	7.2
	(222)	36.969	0.8751	9.6
	(400)	42.950	0.6963	12.3
Fe_3O_4	(111)	18.106	1.6572	4.8
	(220)	29.778	1.1603	7.1
	(311)	35.071	0.9466	8.8
	(440)	42.616	0.7032	12.2

Table 10. The average crystallite size, D_{hkl} (nm) and total means crystallite size, DT (nm) in FI and FC samples.

	D_{hkl} (nm)			D_T (nm)
Sample	Fe	γ-Fe_2O_3	Fe_3O_4	
FI	8.7	8.8	10.0	9.2
FC	8.4	7.9	8.2	8.2

The data of $(\beta_{hkl})_{refined}$ from Si standard sample is shown in Table 7, where this $(\beta_{hkl})_{refined}$ data is actually $(\beta_{hkl})_{instrumental}$. While $(\beta_{hkl})_{refined}$ and D_{hkl} belong to FI and FC samples are shown in Table 8 and 9, respectively, where the crystallite size, D_{hkl} was calculated by using the Equation (3). Table 10 are the average values of D_{hkl} (nm) and the total means crystallite size, D_T (nm) in FI and FC samples.

Appears in Table 10 that the crystallites size in the FC sample is a little bit smaller than the one in FI sample. It means that grinding using the planetary balls milling do change the size of the

crystallites to be smaller than that have previously been established with HEM. Thus, the particles size in FC should also be smaller than the one in FI sample, because a particle may be made up of several different crystallites.

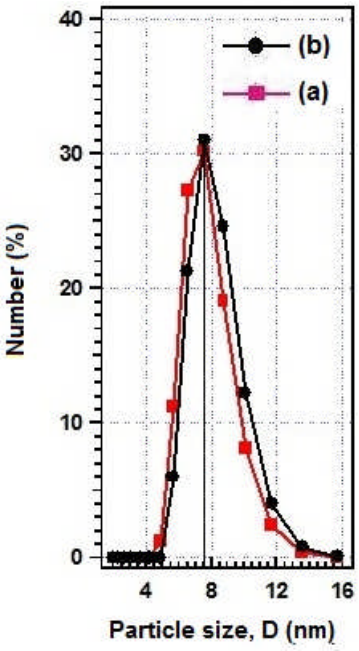

Figure 6. Particle size, and particles size distribution in the samples: FI (a), and FC (b).

That the use of a planetary balls mill is not much to reduce the size of the crystallites is in accordance with previous experiment [17]. Where in that experiment, the high purity iron powder (99.99% pure) with crystallites size of around 550 nm was milled in a planetary balls mill using BTP ratio of 10:1 for a period of 20 h. The average crystallites size decreased to about 270 nm after 20 h of milling. So the size of the crystallites only decrease 51% in a planetary balls mill compared with 99% decreasing that can be achieved by HEM.

The particles size, and its size distribution for the samples of FI and FC were observed by means of PSA. The results, as indicated in Figure 6, show that average particles size in FI and FC are the same of about 7.5 nm. Thus, the function of CTAB as a surfactant that prevent particles from clotting are met. By this milling, it have been produced the particles of around 7.5 nm. While in the last experiment [**7**], the resulting particles ranged from approximately 2 to 4 nm in size. This difference is probably due to the different in BTP weight ratio, which formerly used 10:1 and 5:1 now. The larger the BTP ratio the greater the collisions momentum between balls and powder, so that the mechanical energy induced to the powder to break it into smaller pieces is also greater.

The average crystallites size are larger than the particles size in both FI and FC samples. From this data it can be concluded that the particles size are generally not the same as the size of the crystallites and in particular for the nano-sized particles, the size of crystallites could be equal to or greater than the particles size due to the presence of polycrystalline aggregates [18].

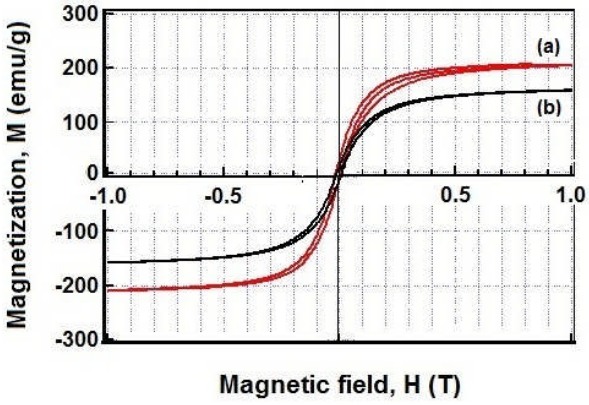

Figure 7. The magnetization curves, M (emu/g) vs applied magnetic field, H (T) at room temperature for the samples: FI (a) and FC (b).

The magnetization curves of magnetic nanoparticles measured at room temperature which were prepared by first and second step milling are shown in Figure 7(a), and (b), respectively. The figures show a typical pattern for soft ferromagnetic or superparamagnetic materials as expected. Unfortunately iron NPs are easily oxidized in air, and the oxidation cause deterioration of their magnetizations. Therefore, for biomedicine applications, iron NPs have to be coated with iron oxide, i.e., γ-Fe_2O_3 or Fe_3O_4 layers.

As shown in Figure 7, the value of the magnetization, M_s decreased from about 204 to 159 emu/g after the second step milling. This is due to the iron-mass fraction decrease from 86% after the first step milling to 67% after the second one. Although the amount of γ-Fe_2O_3 phase increased more than 10 times, but the M_s value of γ-Fe_2O_3 bulk is the smallest compared with the other two phases.

CONCLUSION

This paper, it has been demonstrated a two-steps milling process. The first step, it was carried out a high-energy milling on the Fe powder with the initial size of 10 μm for 40 hours in media isopropyl alcohol. By this milling it was successfully obtained nano particles with an average size of 7.5 nm and crystallites with an average size of 9.2 nm. In the second step, milling was performed using a planetary balls mill in CTAB media. By this milling, the nanoparticles with an average size of 7.5 nm and crystallites with an average size of 8.2 nm have been produced. The two types of sample have equally consisted of Fe, Fe_3O_4 and γ-Fe_2O_3 phases.

For the nano-sized particles, the size of crystallites could be equal to or greater than the size of particles due to the presence of polycrystalline aggregates. Of the magnetization curve, it was revealed that both kind of samples show

superparamagnetic properties, the value of the magnetization decreased after the second step milling due to the iron-mass fraction decrease transforming into iron oxide phases.

ACKNOWLEDGMENTS

The authors thank to the Head of the Center for Science and Technology of Advanced Materials (PSTBM), Drs. Gunawan, M.Sc. and his ranks which have helped to provide research and development facility. To colleagues in PSTBM who can not be mentioned one by one, thanks for their kind help.

REFERENCES

[1]. L. Babes, B. Denizot, G. Tanguy, J.J. Le Jeune and P. Jallet. "Synthesis of Iron Oxide Nanoparticles Used as MRI Contrast Agents: A parametric Study". *Journal of Colloid and Interface Science*, vol. 212, no. 2, pp. 474-482. 1999.

[2]. F.X. Gu, R. Karnik, A.Z. Wang, F. Alexis, E. Levy-Nissenbaum, S. Hong, R.S. Langer and O.C. Farokhzad. "Targeted Nanoparticles for Cancer Therapy." *Nano Today*, vol. 2, No. 3, pp. 14-21. 2007.

[3]. B. Thiesen and A. Jordan. "Clinical Applications of Magnetic Nanoparticles for Hyperthermia." *International Journal of Hyperthermia*, vol. 24, no. 6, pp. 467-474. 2008.

[4]. D. Predoi. "A study on Iron Oxide Nanoparticles Coated with Dextrin Obtained by Coprecipitation." *Digest Journal of Nanomaterials and Biostructures*, vol. 2, no. 1, pp.169. 2007.

[5]. D. Dozier, S. Palchoudhury, and Y. Bao, "Synthesis of Iron Oxide Nanoparticles with Biological Coatings." Internet: http://www.bama.ua.edu/joshua/archive/may10/dozier.pdf , May 23,2013.

[6]. N. Poudyal and J. Ping Liu. "Topical Review: Advances in Nanostructured Permanent Magnets Research." *Journal of Physics D: Applied Physics*, vol. 46, pp. 1-23, November. 2013.

[7]. J. E. Muñoz, J. Cervantes, R. Esparza, and G. Rosas, "Iron Nanoparticles Produced by High-Energy Balls Milling." *Journal of Nanoparticle Research*, vol. 9, Issue 5, pp. 945-950. Oct. 2007.

[8]. Mujamilah, G. T. Sulungbudi, E. Sukirman, Y. Sarwanto dan E. P. Yudho. "Struktur dan Sifat Magnetik Nanopartikel Magnetik (Fe-R) (R:Fe, Tb, Dy, Co) dari Hasil Proses Milling Energi Tinggi." *Jurnal Sains Materi Indonesia*, vol. 13, no. 3, pp. 159-167, Juni. 2012.

[9]. H. Parham, B. Zargar, Z. Heidari and A. Hatamie. "Magnetic Solid-Phase Extraction of Rose Bengal Using Iron Oxide Nanoparticles Modified with Cetyl Trimethyl Ammonium Bromide." *Journal of Iranian Chemistry Society*, vol. 8, pp. S9-S16, Feb. 2011.

[10]. F. Izumi. "Rietan: A Software Package for The Rietveld Analysis and Simulation of X-rays and Neutron Diffraction Patters." *Rigaku Journal*, vol. 6, no. 1, pp. 10-20. 1989.

[11]. P.R. Parmar, M. H. Mangrola, B.H. Parmar, and V.G. Joshi. "A Software to Calculate Crystalline Size by Debye-Scherrer Formula Using VB.NET." *Multi Disciplinary Edu Global Quest (Quarterly)*, vol. 1, Issue 1, p. 147, Jan. 2012.

[12]. "Crystallography Open Data Base." Internet: http://www.crystallography.net/search.html , Jun. 4, 2013.

[13]. Matteo Leoni. "Can Anyone Clarify The Difference Between Grain Size Particle Size and Crystallite Size". Internet: http://www.researchgate.net/post/ , April 28, 2013.

[15]. Bruker Axs GmbH. Internet: http://dcssi.istm.cnr.it/Sironi/didattica/MicroStructura.htm , April 28, 2013.

[16]. Tamilarasan Palanisamy. "Can Anyone Clarify The Difference Between Grain Size Particle Size and Crystallite Size". Internet: http://www.researchgate.net/post/Can April 28, 2013.

[17]. R.K. Khatirkar and B.S. Murty. "Structural Changes in Iron Powder During Balls Milling." *Materials Chemistry and Physics*, vol. 123, pp.247-253, April. 2010.

[18]. T. Ungar and J. Gubicza. "Nanocrystalline Materials Studied by Powder Diffraction Line Profile Analysis." *Z. Kristallographie*, vol. 222, pp. 114-128, 2007.